Electrospun composite membranes for fouling and biofouling control

Berta Díez, Georgiana Amariei, Roberto Rosal. Electrospun composite membranes for fouling and biofouling control. Industrial & Engineering Chemistry Research, 2018, 57, 43, 14561–14570, https://doi.org/10.1021/acs.iecr.8b04011

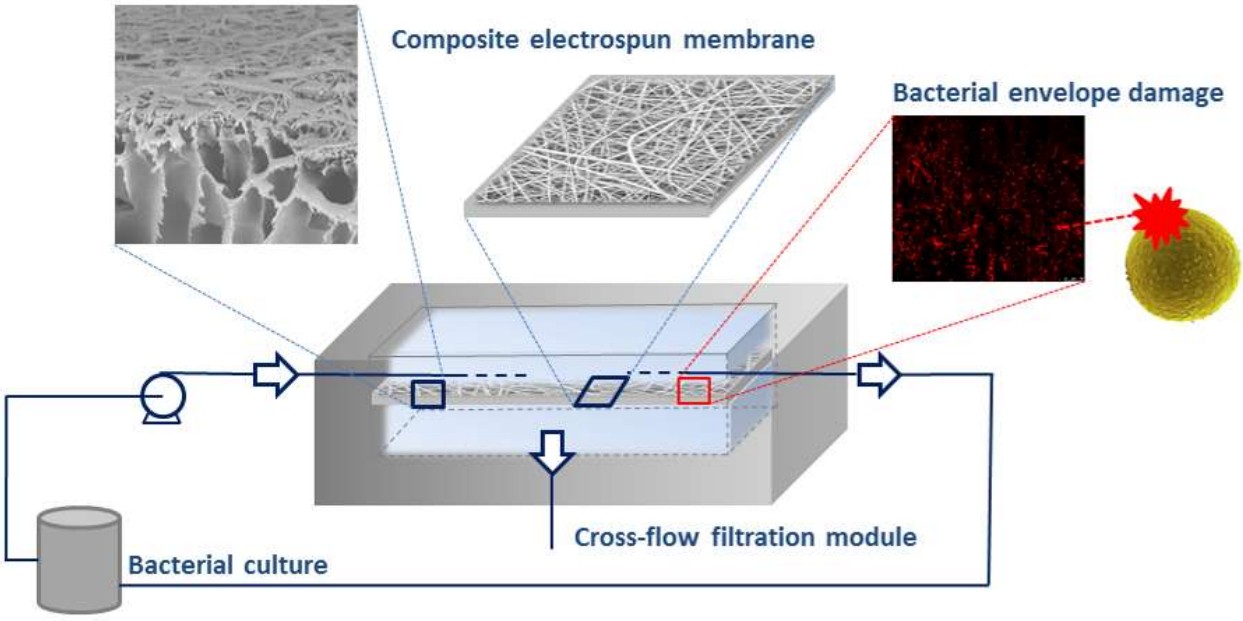

Electrospun composite membranes for fouling and biofouling control

Berta Díez[†], Georgiana Amariei[†], Roberto Rosal[*]

Department of Chemical Engineering, University of Alcalá, E-28871 Alcalá de Henares, Madrid, Spain

[†] Equally contributing authors

[*] Corresponding author: roberto.rosal@uah.es

Abstract

We prepared composite ultrafiltration membranes by directly electrospinning a top layer of poly(acrylic acid) (PAA) and poly(vinyl alcohol) (PVA) onto polysulfone (PSU). The electrospun layer was crosslinked by heat curing and the previous irradiation of the PSU support allowed creating stable composites that did not detach under cross-flow operation. The physicochemical properties of the composites were measured using FTIR spectroscopy, water contact angle, surface ζ-potential and permeation measurements. We showed that PAA-PVA electrospun layers increased membrane hydrophilicity and reduced organic fouling without affecting permeability and protein rejection performance. The antibacterial performance of the top-layer composites was investigated using *Escherichia coli* and *Staphylococcus aureus* strains and tracked counting colony forming units, SEM images of colonized specimens, and cell viability using confocal microscopy. The results showed that PAA-PVA coating resulted in clear antimicrobial performance, particularly for the bacterium *S. aureus*, which we attributed to the chelating of the cations stabilizing cell envelopes. Composite membranes were compared with neat PSU membranes in 48 h cross-flow experiments. The composites showed good mechanical integrity and antimicrobial behavior under flow conditions with average reduction of 1-log for electrospun composites exposed to *S. aureus* over PSU. This work demonstrates that top-layer nanofiber composites can lead to ultrafiltration membranes with enhanced functionalities.

Keywords: Surface modification; Interfacial crosslinking; Electrospinning; Membranes; Biofouling.

1. Introduction

Membrane technology plays a leading role in providing a sustainable use of water and energy resources because of its better efficiency compared to other approaches [1, 2]. Ultrafiltration (UF) is membrane process suitable for large volume operations such as feed pretreatment of reverse osmosis desalination units or the removal of colloids and microorganisms from reclaimed wastewater [3, 4]. Polysulfone (PSU), polyethersulfone (PES), and polyvinylidene difluoride are widely used for producing UF membranes due to their high mechanical and chemical resistance [5]. However, the membranes prepared from these materials are prone to suffer the deposition of nonpolar solutes due to hydrophobic interactions [6]. As a consequence, permeate flux, separation efficiency and membrane lifetime decline during operation [7, 8]. The approaches proposed to limit the adsorption of organic solutes on ultrafiltration membranes include surface functionalization treatments and the use of blending additives to improve surface hydrophilicity or pore architecture [9-12].

Biofouling is the biotic form of organic fouling that describes the accumulation of microorganisms on membrane surface [13]. Biofouling decreases membrane permeability, reduces membrane performance and supposes a risk of pathogen dissemination [14]. Once attached to a surface, microorganisms tend to originate biofilms in which cell communities grow protected by an extracellular polymeric matrix acting as defense against adverse conditions that makes their eradication a very difficult task [15, 16]. The strategies followed to prevent or limit membrane biofouling include the use of disinfecting agents and the design of low-biofouling surfaces [17, 18]. The use of antimicrobial nanoparticles to decorate the active layer of membranes or incorporated into the casting solution has also been explored [19-21].

Electrospinning is a electrohydrodynamic technique suitable for the production of submicron polymeric fibers in which a jet of fluid is charged by a high voltage power source and flows of a capillary tube when the electrostatic force overcomes fluid surface tension [22]. During the path to a grounded electrode, the solvent evaporates, and the solid fiber is collected as non-woven mat or as an ordered array of fibers depending on the collector geometry [23]. The fabrication of electrospun submicrometric fibers have received increased attention in recent years due to the many potential uses of nanofibers in diverse fields [24]. Their main advantages are a high surface to-volume ratio, the versatility to produce different materials via chemical modification, and the creation of coaxial structures [25, 26].

The incorporation of high porosity nanofiber layers onto conventional ultrafiltration membranes has been explored to improve fouling resistance, which was tentatively attributed to the decreased contact time between protein and filtrating layer [27]. A similar approach consisting of placing electrospun nonwovens

onto commercial scaffolds was able to create ultrafiltration composites from microfiltration fabrics [28]. Nanofibrous composites have also been prepared from electrospun polyethylene terephthalate and polyacrylonitrile nanofibers acting as support layer of thin active coatings with the purpose of increasing membrane resistance or water permeability [29, 30]. The replacement of UF layer in conventional thin-film membranes by electrospun nanofibrous membranes has also been explored to provide improved flux [31]. Additionally, electrospun polymeric substrates have been proposed as low tortuosity porous layer in thin film composite nanofiltration membranes with improved permeability [32].

The purpose of this work was to create composite ultrafiltration membranes by directly electrospinning a top layer onto the surface of PSU ultrafiltration membranes, which were previously irradiated to create anchoring points. The polymers chosen were poly(acrylic acid) (PAA) and polyvinyl alcohol (PVA). Both are water-soluble polymers that can be easily crosslinked to produce insoluble materials [33]. Besides, it has been shown that PAA-containing nanofibers fibers exhibit important antibacterial activity attributed to the quelation of the divalent cations stabilizing bacterial envelopes [34, 35]. The composites were characterized using SEM spectroscopy, FTIR, water contact angle (WCA), surface ζ-potential and permeation measurements. The antibacterial and antibiofilm behavior was studied using the bacteria *Escherichia coli* and *Staphylococcus aureus*.

2. Materials and methods

2.1. Chemicals

Polysulfone (PSU, molecular weight 60 kDa) and 1-methyl-2-pyrrolidone (NMP) were obtained from Acros Organics. Polyvinylpyrrolidone (PVP, molecular weight 40 kDa), poly(vinyl alcohol) (PVA, molecular weight 89-98 kDa) and Poly(acrylic acid) (PAA, molecular weight 450 kDa) were acquired from Sigma-Aldrich. Dimethyl sulfoxide (DMSO, 99.9%) and Bovine Serum Albumin (BSA) were obtained purchased from Sigma-Aldrich. Aldrich. Live/Dead BacLight kit and FilmTracer FM 1-43 Green Biofilm Stain were purchased from Invitrogen (Thermo-Fisher, Waltham, USA). Ultrapure water with a resistivity of 18.2 MΩ cm was produced by a Direct-Q™ 5 Ultrapure Water Systems (Millipore, USA) The components of culture media were purchased from Laboratorios Conda (Spain).

2.2. Preparation of electrospun composite membranes

The composite membranes were created by electrospinning a layer of PAA-PVA nanofibers on the top surface of PSU ultrafiltration membranes and are named in what follows as PAA-PVA[number]@PSU, where number refers to the weight density of electrospun layer as indicated in Table 1 and PAA-PVA@PSU refers to any of the composites. The support membranes were ultrafiltration membranes prepared using phase inversion from a casting solution containing 5 wt% PVP and 15 wt% PSU with NMP as solvent. The casting solution was stirred until total dissolution and kept at least 24 hours at room temperature. Once the homogenous solution was prepared, the films were cast to 200 μm thickness using an automatic film applicator AB3120 (TQC, The Netherlands). The prepared films were immediately immersed in a coagulation bath of distilled water for phase separation. The membranes were rinsed in distilled water for at least 24 hours before drying. For a set of membranes, and prior to the electrospinning process, the surface of PSU membranes was functionalized with UV light using a crosslinker equipped with 254 nm lamps. The irradiation time was set at 5 min, which was enough to obtain a clear FTIR carbonyl band at 1710 cm^{-1} (Fig. S2, SI) without compromising the integrity of the skin layer. The latter was assessed by the absence of significant permeability changes and BSA rejection over PSU non-treated membranes. The purpose was to provide anchoring points for the reaction with carboxyl or hydroxyl groups of the electrospun fibers to ensure enough mechanical resistance for the electrospun composite [36].

The coating step with PAA-PVA nanofibers was performed by electrospinning on the top of the skin layer of PSU membranes hold on the grounded collector. The electrospinning solution consisted of PAA (100 mL, 8 wt%) and PVA (11 mL, 15 wt%) in ultrapure water. The solution containing PAA and PVA was stirred (2 h) and degassed before being electrospun. Details on the electrospinning process and parameters can be found elsewhere [35]. The electrospinning time was set to less than 90 min, which corresponded to < 2 mg/cm^2 for the membranes with higher PAA-PVA loadings as indicated in Table 1. This was consistent with the purpose of creating a layer functionalizing the outer surface of the ultrafiltration membrane that did not introduce additional hydraulic resistance or microfiltration functionality. The electrospinning apparatus consisted of a Glassman DC power connected to the needle tip and the grounded collector. The collector was a flat piece of steel covered with aluminum foil in which specimens of the PSU membranes prepared as described previously were carefully placed with the skin layer outwards. The electrospun membranes were dried (50 °C, 24 h) after which, they were crosslinked at 140 °C (30 min), washed with ultrapure water and vacuum-dried (50 °C, 24 h). The whole preparation process is synthesized in the scheme shown in Fig. S1 (Supporting Information, SI).

2.3. Membrane characterization

Attenuated Total Reflectance Fourier Transform Infrared (ATR-FTIR) spectra were recorded using a

Thermo-Scientific Nicolet iS10 equipment. The surface morphology of membranes was studied by scanning electron microscopy (SEM) in a Zeiss DSM-950 apparatus operating at 25 kV on gold-coated samples. The surface charge of membranes was determined by electrophoretic light scattering in a Zetasizer NanoZS apparatus equipped with a ZEN 1020 Cell (Malvern Instruments, UK). The measurements consisted in determining the electrophoretic mobility of a tracer (0.5 wt% PAA, 450 kDa) as a function of the distance to the surface of specimens glued to the sample holder. Further details are given elsewhere [37]. Water contact angle (WCA) was used to determine surface membrane hydrophilicity. Measurements were performed using the sessile drop technique in a Krüss DSA25 equipment at room temperature. At least four drops in different positions were taken for each measurement. The content of carboxyl groups in composite membranes was measured by titrating deprotonated samples with hydrochloric acid under inert atmosphere.

2.4. Membrane filtration performance

Pure water flux, protein rejection and water flux recovery ratio were measured under continuous flow conditions by means of a cross-flow cell module with 20 cm^2 (40 mm x 50 mm) membranes of connected to a 2 L vessel. Membrane permeation flux was determined for transmembrane pressure (TMP) in the 1-4 bar range. Four specimens of each membrane were tested and all of them were maintained in distilled water during 24 h and compacted for at least 30 min at 4 bars at room temperature before measurements. Fouling measurements were performed using BSA as a model for protein rejection. BSA solution 1 g L^{-1} prepared in phosphate-buffered saline (PBS, 0.1 M, pH 7.2) was used for fouling assays, which were performed at 2 bar TMP, and 0.80 m s^{-1} linear velocity. Pure water filtration and BSA filtration experiments were performed to evaluate water fluxes, J_w^i, before and after BSA filtration followed by membrane cleaning at zero transmembrane pressure for at least 30 min, J_w^f.

The experiments with BSA were conducted the time required to filter 0.5 g/cm^2 BSA. Flux recovery ratio (FRR) was calculated according to the following expression:

$$FRR(\%) = \left(\frac{J_w^f}{J_w^i}\right) \times 100 \qquad [1]$$

FRR represents the irreversible fouling and the part of the reversible fouling due to the formation of a cake layer (excluding concentration polarization). Solute rejection, R, was determined from BSA concentration in permeate and feed, *Cf* and *Cp*, respectively, measured from UV absorbance at 261 nm in a Shimadzu SPD-6AV spectrophotometer:

$$R(\%) = \left(1 - \frac{C_p}{C_f}\right) \times 100 \qquad [2]$$

2.5. Antimicrobial effect and antibiofouling behaviour

Neat PSU and PAA-PVA@PSU composites were tested for their antibacterial activity against two different microbial strains, the gram-positive bacterium *S. aureus* (CECT 240, strain designation ATCC 6538P) and the gram-negative bacterium *E. coli* (CECT 516, strain designation ATCC 8739). The microorganisms were reactivated using nutrient broth (NB) at pH 7.0 ± 0.1 and 36 °C under agitation (250 rpm) and followed by optical density (OD) at 600 nm. For the antimicrobial runs, NB was diluted 500-fold. The antimicrobial effect of composite membranes was evaluated by determining Colony-Forming Units (CFU) under static and cross-flow conditions as prescribed in ISO 22196 with minor modifications.

For the static test, dried membranes in accurately weighed pieces were placed into sterile 24-well plates with neat PSU membranes as negative controls. A bacterial suspension was prepared by diluting 0.4 mL of a 10^6 cell/mL cultures in 2.0 mL NB 1/500, which was added into the each well and incubated for 20 h at 36 °C. After exposure, the membranes were washed with PBS and shaked 10 min at 5 °C to remove non-adhered cells. Adhered cells were recovered using SCDLP (soybean casein digest broth with lecithin and polyoxyethylene sorbitan monooleate) following ISO 22196. The supernatant liquid after 20 h exposure and the suspension resulting from cell detachment were serially diluted in PBS and colony counting performed after inoculation of Petri dishes containing NB and incubation at 36 °C for 16 h. At least 3 replicates of at least two serial dilutions were used for each sample and all experiments were replicated until obtaining sufficient accuracy.

In the cross-flow device, the antimicrobial effect of composite membranes was tested by checking specimens with the maximum amount of PAA-PVA against the growth of S. *aureus*. For it, neat PSU and PAA-PVA@PSU composites were located in the cross-flow module and connected to the feed flask that contained an initial bacterial concentration of 10^6 cells/mL in diluted nutrient broth medium (NB 1/500) at 25 °C. Before every experiment and the cross-flow unit was carefully cleaned and disinfected using a method adapted from Jeong et al. [38]. Briefly, 0.5% sodium hypochlorite was circulated for 2 h followed by twice water rinsing for 10 min. Afterwards, trace organic matter was removed by circulating 5 mM EDTA, pH 11, for 30 min, followed by water rinsing and 2 mM sodium dodecyl sulphate, pH 11, for 30 min, followed by new water rinsing. Sterilization was performed by autoclaving the entire unit at 121 °C for 2 h. The connecting tubes were also sterilized as described previously [39]. After 48 h samples from the retentate were collected and CFU counted according to the procedure describe before. 48 h was set as a practical limit because the device could not be stopped

or left unattended. The membranes were then removed, carefully washed in PBS and incubated in SCDLP medium to detach the bacterial and determinate the number of viable cells attached to the membrane surface.

Bacterial viability was assessed by means of Live/Dead BacLight Bacterial Viability kit (Molecular Probes). The method is based on two fluorescent nucleic acid probes, one of which, SYTO9, penetrates intact cell membranes marking viable cells in green, while the other, propidium iodide (PI), is only internalized by membrane-damaged cells, that become red-stained. Confocal micrographs were taken in a fluorescent microscope Leica Microsystems SP5.

Cell bodies on membrane surface were visualized by means of FilmTracer FM 1-43 Green Biofilm Cell Stain used as indicated by the manufacturer. Stained cells were visualized by confocal laser microscopy (LEICA TCS-SP5) using an excitation/emission maxima wavelength of 472/580 nm. The non-fluorescent water-soluble dye inserts into the surface of bacterial membranes where they become intensely fluorescent. The formation of biofilms onto membrane surface was also assessed by SEM using membrane specimens previously cleaned, fixed and dehydrated.

3. Results and Discussion

3.1. Membrane characterization

The properties of base and irradiated PSU membranes and the electrospun PAA-PVA@PSU composites are shown in Table 1. Specimens PAA-PVA[1]@PSU to PAA-PVA[4]@PSU were prepared onto non-irradiated PSU membranes, while membranes designated as PAA-PVA[5]@PSU to PAA-PVA[8]@PSU corresponded to the higher coating coverage of the electrospun top layer. Irradiated PSU membranes, marked as "+" in Table 1 were UV treated for 5 min. The reason for this procedure was that PAA-PVA loadings above 0.1 mg cm^{-2} tended to detach from non-irradiated PSU base membranes when running 24 h experiments in cross-filtration regime (2 bar TMP, linear velocity 0.80 m s^{-1}) as shown by visual inspection of micrographs. However, pre-irradiated membranes kept fibers attached to the PSU membrane for all tested loadings (up to 1.85 mg cm^{-2}). Crosslinking treatment (30 min, 140 °C) was used to stabilize the electrospun layer rendering water insoluble composites. The electrospun PAA-PVA layers deposited and crosslinked onto irradiated supports preserved their fibrous structure after 48 h in all cases, the stability being attributed to the interaction between PAA-PVA moieties and oxygenated groups from the surface of irradiated PSU [40]. Accordingly, WCA decreased for irradiated PSU membranes as shown in Table 1. Membrane surface charge measured using surface ζ-potential at pH 7.0 is also shown in Table 1. Surface charge was negative in all cases with more negative values for PAA-PVA composite membranes, and even more negative for increasing amounts of the electrospun layer up to a value as low as -41.2 ± 0.13 mV. Uncoated PSU displayed negative charge, with ζ-potential -30.1 ± 1.8 mV. The negative charge of PSU membranes, that does not contain charged groups, is usually explained by the adsorption of hydroxide ions on membrane surface [41]. The reason for the more negative charge of PAA-PVA loaded composites was the presence of carboxylate moieties in the PAA backbone [35]. Membrane surface hydrophilicity was studied by measuring the WCA between the membrane surface and the air–water interface. The values obtained are also presented in Table 1. WCA decreased for increasing amounts of the electrospun layer, which can be explained by two factors. First, because of the presence of hydrophilic groups in PAA-PVA polymeric fibers. Second, because surface roughness decreases the measured contact angles in hydrophilic surfaces (and increases in hydrophobic surfaces) from the values measured in the chemically identical flat surfaces.

Table 1. Properties of the synthesized composites. (The intervals represent standard deviation.)

Membrane	UV[a]	Weight density of fibers (mg/cm^2)	Surface ζ-potential (mV) at pH 7	Water contact angle (WCA °)	-COOH (mmol/g)
PSU	-	—	-30.1 ± 1.8	65.3 ± 3.1	0.0 ± 0.5
PSU[0]	+	—	-29.3 ± 0.4	60.1 ± 0.8	0.0 ± 0.6
PAA-PVA[1]@PSU	-	0.03 ± 0.01	-31.9 ± 0.6	65.5 ± 0.9	0.9 ± 0.1
PAA-PVA[2]@PSU		0.04 ± 0.02	-31.6 ± 0.9	62.6 ± 1.3	2.9 ± 1.4
PAA-PVA[3]@PSU		0.05 ± 0.01	-31.1 ± 2.8	58.8 ± 1.4	4.1 ± 0.1
PAA-PVA[4]@PSU		0.12 ± 0.03	-33.5 ± 2.8	55.6 ± 1.1	4.2 ± 0.1
PAA-PVA[5]@PSU	+	0.46 ± 0.07	-35.2 ± 3.8	52.1 ± 4.2	5.8 ± 0.1
PAA-PVA[6]@PSU		0.83 ± 0.19	-37.1 ±1.9	48.2 ± 3.3	8.5 ± 0.2
PAA-PVA[7]@PSU		1.18 ± 0.28	-38.1 ± 1.4	43.8 ± 0.9	8.9 ± 0.3
PAA-PVA[8]@PSU		1.85 ± 0.32	-41.2 ± 0.1	39.0 ± 1.7	11.6 ± 0.2

[a] "-" represents composites prepared from non-irradiated PSU membranes, "+" represents UV-treated base membranes.

Fig. 1 shows the ATR-FTIR spectra of the outer layer of uncoated PSU and PAA-PVA@PSU composites. For the PSU membrane, the bands at 1585, 1504, 1489 and 1100 cm^{-1} are due to the vibrations of PSU aromatic ring (C=C stretching). The peak at 1244 cm^{-1} corresponds to the PSU aromatic ether bond (–C–O–C–), while the weak stretching vibrations of the C–H bonds of PSU was observed in the 2860-2900 cm^{-1} region [42]. Most new peaks appearing in the composite membrane are characteristic of the PAA-PVA coating such the C–H alkyl stretching vibration (2850–3000 cm^{-1}). The characteristic carboxyl stretching band of PAA appears at 1700 cm^{-1}. The symmetric and antisymmetric stretching of carboxylate ion (COO-) appeared at 1420 cm^{-1}[43]. The formation of anhydride and ester moieties during heat curing of PAA-PVA blends was assessed elsewhere by tracking the decrease of the C=O stretching vibration and the growth of the C-O-C stretching bands, observed here at 1165 cm^{-1}[35, 44]. The IR spectrum of the composite samples with lower amount of polymeric coating was dominated by the bands attributed to PSU, which decreased for higher PAA-PVA loadings as the surface of the composite material became covered by the polymeric electrospun layer.

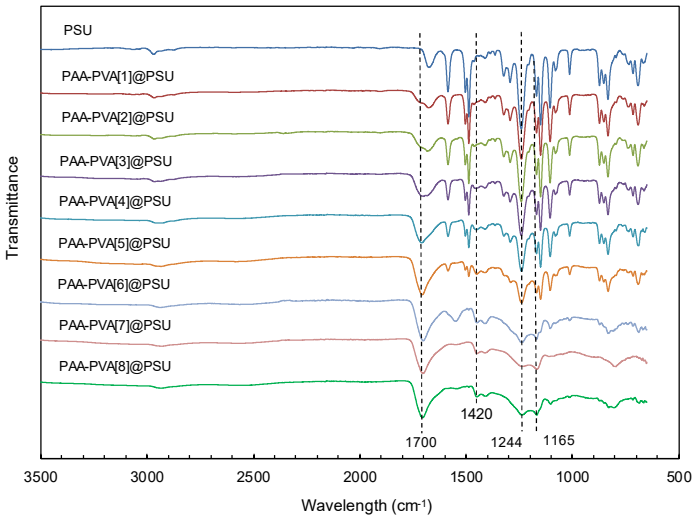

Figure 1. ATR-FTIR spectra of PAA-PVA@PSU composite membranes.

ATR-FTIR spectra irradiated, and non-irradiated PSU membranes are shown in Fig. S2 (SI). PSU irradiated membranes showed a clear OH stretching band at 3400 cm^{-1} and a broad band at 1725 cm^{-1} due to the C=O stretching of carboxyl groups. The changes can be explained by the oxidative photolysis of aromatic moieties [45]. The broad band at 1500-1900 cm^{-1} corresponded to carbonyl (C=O) groups, the band in the 2500–3700 cm^{-1} region was due to the presence of hydroxyl groups, and the band at 1100-1350 cm^{-1} region was due to C-O single bonds [46]. The decrease observed in the band at ~1325 cm^{-1}, due to bond scissions of C-O and C-S (Fig. S2, SI) agreed with the formation of common photoproducts of the diphenylethersulfone units [47].

The morphology of composite membranes is shown in Fig. 2 as a series of surface SEM images of representative specimens. Figs. 2a-c corresponds to the upper view of membranes prepared with different PAA-PVA loadings after heat curing. The images indicated that PAA-PVA electrospun material formed a continuous layer on top of the PSU support consisting of well-formed fibers without beading or other flaws that kept their fibrous structure after heat curing. Fig. S3 (SI) shows a complete set of upper view SEM micrographs before and after heat curing and after water conditioning. The electrospun layer preserved its fibrous structure after 24 h water immersion and did not detach from the support. The average diameter of fibers in the electrospun layer was 220 ± 50 nm that increased after water immersion to 440 ± 80 nm due to the swelling behavior of the polymeric material [48]. Figs. 2d-f show cross-sectional SEM images of PSU and composite membranes. Fig. 2d corresponds to neat PSU and displayed the usual asymmetric structure with a top skin layer over a porous substrate. Composite specimens (Figs. 2e and 2f) exhibited similar morphological structure with a well-developed layer of electrospun fibers with a thickness in the few microns range.

3.2. Filtration performance

The results of water permeability for composite PSU membranes are shown in Fig. 3 that shows a slight increase in water permeability as the weight load of PAA-PVA increased. Irradiation treatment resulted in a slight increase of water permeability compatible with the higher surface polarity. The permeability of composite specimens also increased slightly with the incorporation of the electrospun layer. The results showed that the incorporation of the electrospun layer did not add an important additional hydraulic resistance and, therefore, the pores of the skin ultrafiltration layer did not become blocked by the electrospun material with only a slight decrease in permeability from irradiated membranes, PSU(o), to the composite specimens PAA-PVA[5-8]@PSU prepared using irradiated supports. This result suggests that neither the pore structure of the skin layer was affected by the electrospun material. The enhancement of membrane permeability obtained by the use of polymeric mixtures or blending additives is due to the more hydrophilic pores that interact with water molecules and facilitate water flux [49]. Accordingly, significant changes in water permeability were not expected.

Membrane fouling was studied in cross-flow mode by filtering 1 g L^{-1} BSA aqueous solution in rejection experiments conducted at 2 bar TMP. The rejection was studied for neat PSU and composites membranes covered with different amount of PAA-PVA

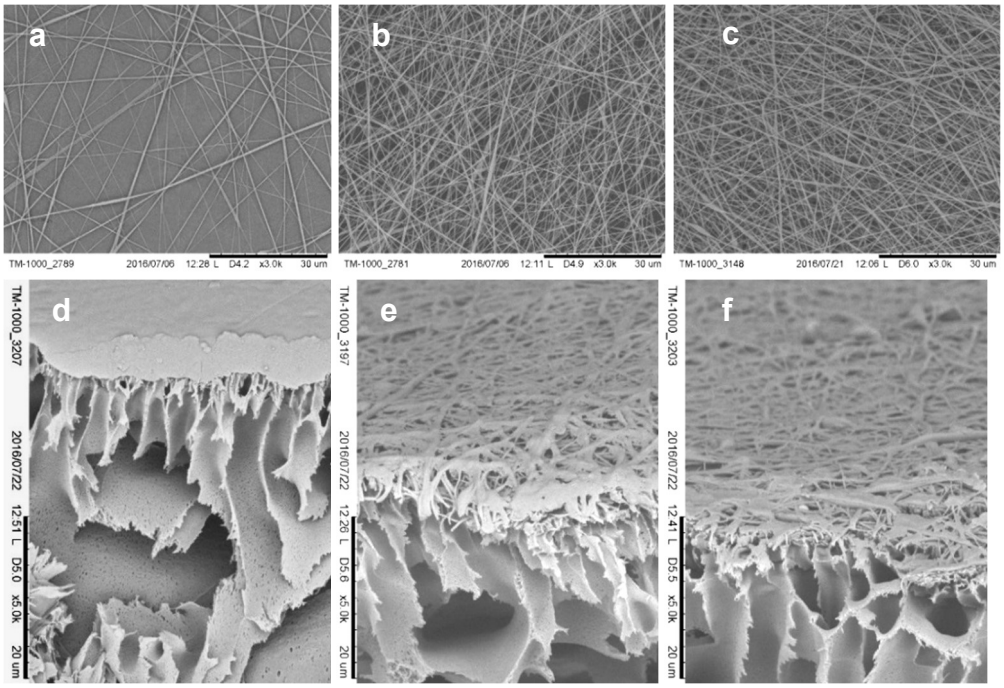

Figure 2. Upper row: SEM images of composite membranes in upper view: (a) PAA-PVA[1]@PSU, (b) PAA-PVA[5]@PSU and (c) PAA-PVA[8]@PSU. Lower row: Cross-sectional SEM images of (d) neat PSU, (e) PAA-PVA[5]@PSU and (f) PAA-PVA[8]@PSU.

nanofibres. The results were very similar (> 90%) for protein rejection in all the tested specimens ranging from 93.5 ± 0.7 % (PSU) to 95.5 ± 0.6 % for the highest PAA-PVA coverage (Fig. 3). Consequently, the incorporation of the electrospun top layer of PAA-PVA did not affect protein retention as expected considering the base PSU membrane bearing the ultrafiltration layer was the same. The fact that membranes prepared from irradiated supports did not show significant deviations with pristine PSU is an additional proof of the lack of degradation upon UV exposure.

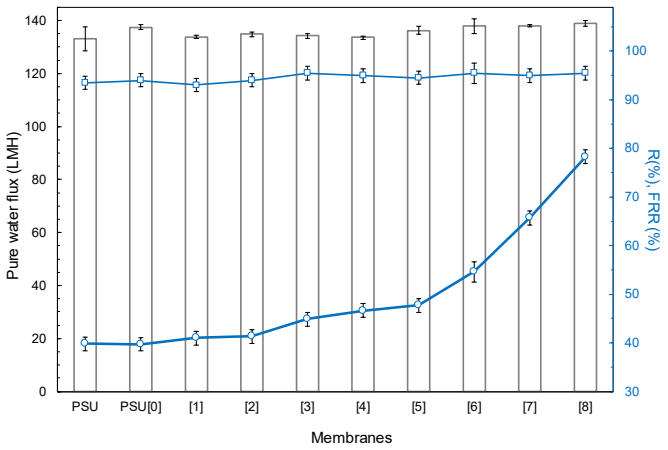

Figure 3. Pure water flux (bars), BSA rejection ratio (R, □) and flux recovery ratio (FRR, ○) for the tested membranes. The numbers refer to the nomenclature explained in Table 1. Error bars represent standard deviation.

The antifouling performance was determined by measuring the water flux decline before and after filtration of BSA solution (Eq. 1). The results, also shown in Fig. 3, indicated that the presence of the electrospun layer increased the flux recovery ratio with the amount of PAA-PVA nanofibres. The maximum loading of the electrospun layer resulted in flux recovery ratio of 78.3 ± 0.3 % contrasting with 39.8 ± 0.2 % for neat PSU membranes. The reduction of organic fouling (irreversible plus cake layer) by 38.4 % can be exclusively attributed to the incorporation of the layer of electrospun PAA-PVA fibers onto the PSU base membranes. The increase of membrane hydrophilicity is a well-known way of reducing membrane fouling due to a lower interaction with colloidal, and biological species[50, 51]. Another effect contributing to the antifouling performance of composite membranes is the electrostatic repulsion between top layer membrane and negatively charged substrates, which is the case of BSA, negatively charged at pH 7 (ζ-potential -15 ± 3 mV) and with isoelectric point 4.7-4.9 [52]. Surface roughness could result in the retention of particles that could fit into the microsized pores of the electrospun material. This would be the case of bacteria and other colloids. However, the negative charge of the top layer would contribute to exclude negatively charged solutes, which are by far the most commonly found in wastewater.

3.3. Antimicrobial performance

Fig. 4 shows the results of microbial growth tests. Fig. 4a for membranes kept in contact with *E. coli* and Fig. 4b for *S. aureus*. In all cases, the initial microbial load was 6.7 x 10^4 cells/mg and the incubation took place for 20 h at 36 °C. After the incubation period the cells attached to membranes were removed as explained before and the resulting liquid plated in serial dilutions

for viable cell counting. CFU counting for the culture liquid in contact with membranes after separating it from membranes at the end of the exposure experiment is shown in Fig. S4 (SI). The results revealed a considerable impairment for both bacteria, with > 1-log reduction (1-log represents 90% reduction) for *S. aureus* growth on membrane surface and 2.5-log reduction in the medium in contact with membranes. The corresponding figures for *E. coli* were < 1-log for cells detached from the surface and 1.8-log reduction for the liquid culture medium. The antimicrobial effect of PAA containing polymers has been attributed to the chelation of the cations stabilizing bacterial envelopes, based on measurements of bacterial surface charge and intracellular calcium [35, 53]. The role of PAA as calcium chelator is also explained by theoretical findings showing that the sequestration process is spontaneous due to the increase in entropy rather than to electrostatic forces [54]. Further experimental evidence demonstrated that the binding constant of calcium to the bacterial cell wall was high enough to allow the removal of calcium as Ca-PAA complexes [55].

Fig. 4 also shows that *S. aureus* was considerably more impaired than *E. coli* after exposed to PAA-PVA@PSU composites. For the case of *S. aureus*, the specimens with 0.05 mg/cm^2 electrospun layer already displayed a significant antimicrobial effect, whereas for *E. coli* the effect was only clear at loadings of 0.46 mg/cm^2 or higher. (The asterisks in Fig. 4 indicate results significantly different from PSU controls.) For *S. aureus*, the decrease of CFU in the liquid in contact with membranes was over 2-log compared to PSU controls, a result that can be attributed to the tendency of both strains to form biofilms. The external differences between *S. aureus* and *E. coli* explain the different effect based on their cell wall structures. The outer membrane of *E. coli* is a lipid bilayer that includes a complex lipopolysaccharide leaflet, which include phosphate groups electrostatically balanced with divalent cations that stabilize the assembly [56]. The removal of such cations from the outer envelope of gram-negative bacteria by PAA affects membrane integrity by breaking the interlocking of lipopolysaccharide molecules. *S. aureus*, however, is a gram-positive bacterium, that instead of an outer membrane possesses a thick peptidoglycan layer [57]. The phosphate groups of teichoic acid and the negatively charged moieties of peptidoglycan provide a net negative charged surface that requires cationic counterions to provide membrane integrity. It was

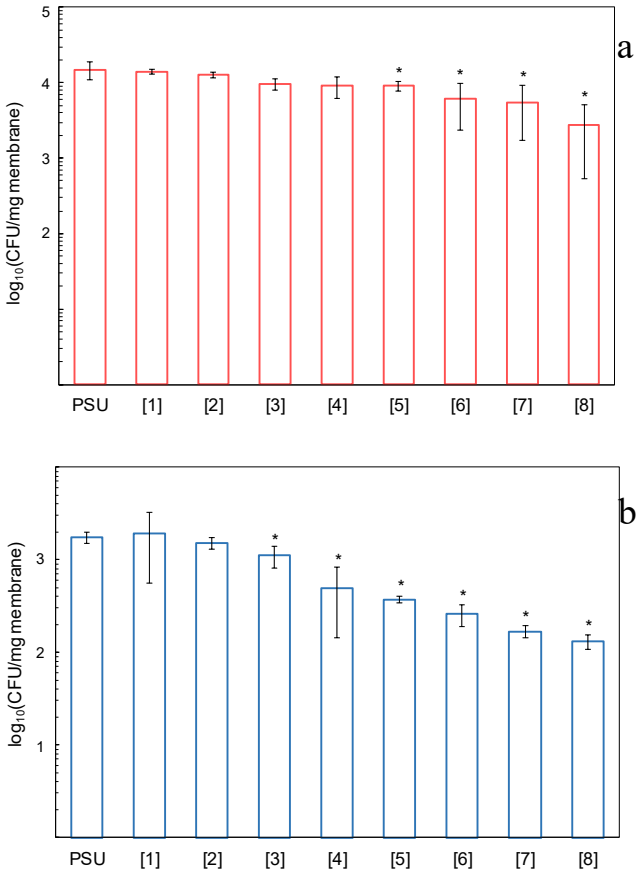

Figure 4. Colony-forming units (CFU) for microorganisms detached from membranes exposed to (a) E. coli and (b) S. aureus. The cultures were kept in contact with bacteria for 20 h at 36 °C. The numbers refer to the nomenclature explained in Table 1. Error bars represent standard deviation.

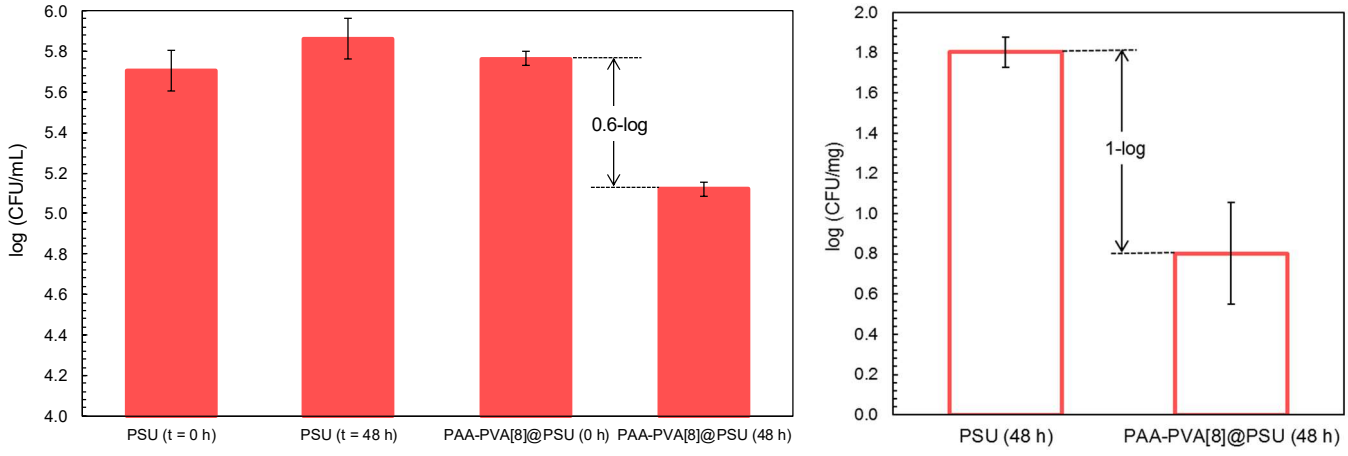

Figure 5. Microbial growth in cross-flow operation for 48 h at 25 °C. Left: CFU in the retentate; right: CFU detached from membrane surface at the end of the exposure period per unit mass of membrane. TMP 2 bar; linear velocity 0.80 m s-1. Error bars represent standard deviation.

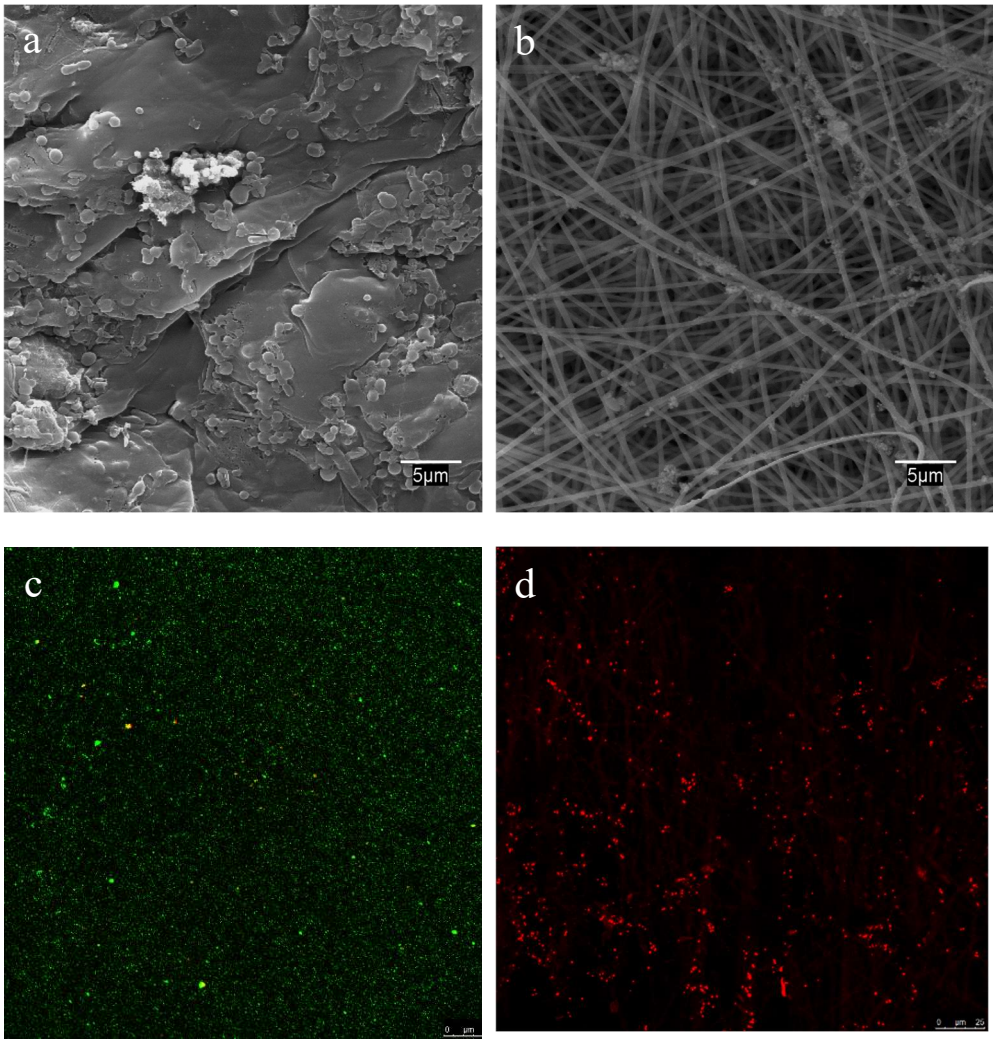

Figure 6. SEM and Live/dead confocal micrographs of PSU and PAA-PVA[8]@PSU membranes after 48 h in cross-flow at 25 °C. Initial bacterial load in circulating feed: 106 cells/mL of *S. aureus* in NB 1/500 medium. SEM micrographs of (a) PSU and (b) PAA-PVA[8]@PSU and Live/Dead confocal micrographs of the surface of (c) PSU and (d) PAA-PVA[8]@PSU.

shown that calcium is the preferred cation for stabilizing the cell wall of gram-positive bacteria [58]. Later, it has been reported that the binding affinity of calcium for peptidoglycan was lower than that for PAA, this being the probable cause for the damage observed upon exposure of bacterial cells to the composite membranes containing PAA [59].

Representative SEM images of composite membranes after exposure to *E. coli* and *S. aureus* are shown in Fig. S5 and Fig. S6 respectively (SI). The SEM images of PSU controls showed large bacterial colonization, which, in the case of *S. aureus* led to membranes covered with bacterial cells Fig. S6a). The presence of adhesion structures and extracellular matrix was clear also for the composite membranes with lower PAA-PVA loadings (Figs.S5 b-c-d and Figs. S6 b-c-d). However, for the specimens with higher amount of PAA-PVA, the surfaces were almost free from bacteria, with dispersed colonization areas probably benefiting from the higher surface roughness of composites [60]. The effect PAA-PVA loadings would be the destabilization of the bacterial wall due to the removal of divalent cations or impairment of lipopolysaccharide interlocking. The effect is also clear for planktonic cells as shown by the lower CFU counts in the liquid in contact with membranes.

Further insight on the colonization of composite membranes was provided by the visualization of biofilm formation by means of FilmTracer FM 1-43. Fig. S7 (SI) shows representative confocal micrographs of membranes exposed to *S. aureus* cultures for 20 h at 36 °C. FM 1-43 is a non-fluorescent water soluble lipophilic compound that inserts into the bacterial membrane where it becomes fluorescent revealing cell bodies even in complex biofilms in which other stains do not reveal cells as they are surrounded by large amounts of exopolymeric substances Fig S7 shows that composite membrane with low PAA-PVA loadings suffered bacterial colonization and biofilm formation, whereas for higher loadings, particularly for PAA-PVA[8]@PSU, the membrane with 1.85 ± 0.32 mg PAA-PVA/cm^2, the surface was considerably more clean than PSU controls.

Control PSU and PAA-PVA[8]@PSU composites were also assayed in 48 h crossflow runs with full filtrate and retentate recirculation at 2 bars TMP and an average

linear velocity of 0.80 m s^{-1} along the membrane surface. The temperature of the assay was reduced from the 36 °C of the previous antimicrobial tests to 25 °C in search for more realistic conditions and due to the operational limitations of keeping a constant temperature in a circulating cross-flow system over a prolonged period of time. The results are shown in Figs. 5 and 6. Fig. 5 shows that CFU increased in the circulating liquid when using a PSU membrane, which became colonized by 63 ± 12 CFU/mg. Instead, the composite membrane with PAA-PVA, PAA-PVA[8]@PSU, was essentially free of bacterial colonization, 1-log less than PSU accompanied by lower CFU in the circulating liquid (0.6-log reduction).

SEM and confocal images of colonized membranes, PSU and PAA-PVA[8]@PSU, after 48 h runs in cross-flow at 25 °C are shown in Fig. 6. SEM images clearly showed extensive biofilm formation in the case of PSU (Fig. 6a). On the contrary, membranes with the PAA-PVA electrospun layer were mostly free of bacteria, with certain colonization but without evidence of the biofilm matrix produced with extracellular substances in the final stages of bacterial colonization (Fig. 6b). The electrostatic repulsion between the outer bacterial envelope and the top layer of composite membranes, could at least partially explain the lower colonization observed [61]. However, the damage observed in bacterial envelopes support the quelation mechanism as the main driver of the antimicrobial activity of the top layer. The electrostatic repulsion between the outer surface of bacteria and the top layer of composite membranes, could at least partially explain the lower colonization observed [61]. However, the damage observed in bacterial envelopes support the quelation mechanism as the main driver of the antimicrobial activity of the top layer. Cell damage is revealed by the confocal Live/Dead images shown in Fig. 6c-d. Using the Live/Dead staining, SYTO9 green-labelled cells correspond to non-damaged bacteria, while PI reveals as red-marked membrane-damaged bacteria. PSU membranes were covered by a considerable amount of viable green-labelled *S. aureus* cells as shown by Fig. 6c. However, Live/Dead confocal images of PAA-PVA[8]@PSU composites under the same conditions showed extensive cell impairment with essentially all cells becoming red-stained Fig. 6d. Red-marked cells were those internalizing PI and damaged in cell membrane integrity. The results are in good agreement with the antimicrobial assays performed in static conditions and show the advantages of using electrospun antimicrobial layers on ultrafiltration membranes to control microbial growth and biofilm formation even under flow conditions.

4. Conclusions

We report the preparation and properties of composite membranes consisting of electrospun layers of poly(acrylic acid)-poly(vinyl alcohol) (PAA-PVA) as top coating of a PSU ultrafiltration membrane. The electrospun layer formed a continuous coating consisting of well-formed fibers that kept their fibrous structure after heat curing and water immersion and did not detach from support.

The composite membranes displayed negative surface charge with more negative values for increasing amounts of the PAA-PVA electrospun layer up to a value of -41.2 ± 0.13 mV for the higher loading for a weight density of 1.85 ± 0.32 mg/cm^2. PAA-PVA composite membranes showed improved resistance to organic fouling with flux recovery ratio up to 80.2 % over the value of 29.4 % for PSU membranes.

Composite membranes showed considerable antimicrobial activity. The effect was larger for *S. aureus* than for *E. coli*, which was attributed to the chelating effect of PAA on the divalent cations stabilizing bacterial envelopes. Viability studies showed that bacterial cells in contact with composite membranes displayed a high number of membrane-damaged bacteria.

The results demonstrated the feasibility of using electrospun layers directly created onto filtration supports as top coatings for ultrafiltration membranes with the aim of improving fouling behavior and imparting antimicrobial functionality.

Acknowledgements

Financial support for this work was provided by the FP7-ERA-Net Susfood, 2014/00153/001 and the Dirección General de Universidades e Investigación de la Comunidad de Madrid, Research Network S2013/MAE-2716. BD and GA thank the University of Alcalá for the award of predoctoral grants.

Author contributions

The manuscript was written through contributions of all authors and all authors have given approval to the final version of the manuscript. BD and GA contributed equally.

References

1. Elimelech, M.; Phillip, W. A. The future of seawater desalination: Energy, technology, and the environment. *Science* **2011,** *333*, (6043), 712-717.
2. Rajasulochana, P.; Preethy, V. Comparison on efficiency of various techniques in treatment of waste and sewage water – A comprehensive review. *Resource-Efficient Technologies* **2016,** *2*, (4), 175-184.
3. Liu, P.; Hill, V. R.; Hahn, D.; Johnson, T. B.; Pan, Y.; Jothikumar, N.; Moe, C. L. Hollow-fiber ultrafiltration for simultaneous recovery of viruses, bacteria and parasites from reclaimed water. *J. Microbiol. Methods* **2012,** *88*, (1), 155-161.
4. Löwenberg, J.; Baum, J. A.; Zimmermann, Y. S.; Groot, C.; van den Broek, W.; Wintgens, T. Comparison of pre-treatment technologies towards improving reverse

osmosis desalination of cooling tower blow down. *Desalination* **2015,** *357*, 140-149.
5. Association, A. W. W. *Microfiltration and Ultrafiltration Membranes for Drinking Water*. 1st ed.; American Water Works Association: Denver, 2005; Vol. 53.
6. Choo, K. H.; Lee, C. H. Understanding membrane fouling in terms of surface free energy changes. *J. Colloid Interface Sci.* **2000,** *226*, (2), 367-370.
7. Le-Clech, P.; Chen, V.; Fane, T. A. G. Fouling in membrane bioreactors used in wastewater treatment. *J. Membr. Sci.* **2006,** *284*, (1), 17-53.
8. Prince, J. A.; Bhuvana, S.; Boodhoo, K. V. K.; Anbharasi, V.; Singh, G. Synthesis and characterization of PEG-Ag immobilized PES hollow fiber ultrafiltration membranes with long lasting antifouling properties. *J. Membr. Sci.* **2014,** *454*, 538-548.
9. Taniguchi, M.; Belfort, G. Low protein fouling synthetic membranes by UV-assisted surface grafting modification: varying monomer type. *J. Membr. Sci.* **2004,** *231*, (1), 147-157.
10. Sotto, A.; Boromand, A.; Zhang, R.; Luis, P.; Arsuaga, J. M.; Kim, J.; Van der Bruggen, B. Effect of nanoparticle aggregation at low concentrations of TiO_2 on the hydrophilicity, morphology, and fouling resistance of PES–TiO_2 membranes. *J. Colloid Interface Sci.* **2011,** *363*, (2), 540-550.
11. Zhao, Y. F.; Zhu, L. P.; Yi, Z.; Zhu, B. K.; Xu, Y. Y. Improving the hydrophilicity and fouling-resistance of polysulfone ultrafiltration membranes via surface zwitterionicalization mediated by polysulfone-based triblock copolymer additive. *J. Membr. Sci.* **2013,** *440*, 40-47.
12. Gao, H.; Sun, X.; Gao, C. Antifouling polysulfone ultrafiltration membranes with sulfobetaine polyimides as novel additive for the enhancement of both water flux and protein rejection. *J. Membr. Sci.* **2017,** *542*, 81-90.
13. Flemming, H. C.; Schaule, G.; McDonogh, R. Biofouling on Membranes — A Short Review. In *Biofilms — Science and Technology*, Melo, L. F.; Bott, T. R.; Fletcher, M.; Capdeville, B., Eds. Springer Netherlands: Dordrecht, 1992; pp 487-497.
14. Flemming, H. C. Biofouling in water systems – cases, causes and countermeasures. *Appl. Microbiol. Biotechnol.* **2002,** *59*, (6), 629-640.
15. de la Fuente-Núñez, C.; Reffuveille, F.; Fernández, L.; Hancock, R. E. W. Bacterial biofilm development as a multicellular adaptation: antibiotic resistance and new therapeutic strategies. *Current Opinion in Microbiology* **2013,** *16*, (5), 580-589.
16. Giaouris, E.; Heir, E.; Hébraud, M.; Chorianopoulos, N.; Langsrud, S.; Møretrø, T.; Habimana, O.; Desvaux, M.; Renier, S.; Nychas, G. J. Attachment and biofilm formation by foodborne bacteria in meat processing environments: Causes, implications, role of bacterial interactions and control by alternative novel methods. *Meat Science* **2014,** *97*, (3), 298-309.
17. Matin, A.; Khan, Z.; Zaidi, S. M. J.; Boyce, M. C. Biofouling in reverse osmosis membranes for seawater desalination: Phenomena and prevention. *Desalination* **2011,** *281*, 1-16.
18. Kochkodan, V.; Hilal, N. A comprehensive review on surface modified polymer membranes for biofouling mitigation. *Desalination* **2015,** *356*, 187-207.
19. Zodrow, K.; Brunet, L.; Mahendra, S.; Li, D.; Zhang, A.; Li, Q.; Alvarez, P. J. J. Polysulfone ultrafiltration membranes impregnated with silver nanoparticles show improved biofouling resistance and virus removal. *Water Res.* **2009,** *43*, (3), 715-723.
20. Yu, H.; Zhang, X.; Zhang, Y.; Liu, J.; Zhang, H. Development of a hydrophilic PES ultrafiltration membrane containing SiO2@N-Halamine nanoparticles with both organic antifouling and antibacterial properties. *Desalination* **2013,** *326*, 69-76.
21. Díez, B.; Roldán, N.; Martín, A.; Sotto, A.; Perdigón-Melón, J. A.; Arsuaga, J.; Rosal, R. Fouling and biofouling resistance of metal-doped mesostructured silica/polyethersulfone ultrafiltration membranes. *J. Membr. Sci.* **2017,** *526*, 252-263.
22. Reneker, D. H.; Yarin, A. L. Electrospinning jets and polymer nanofibers. *Polymer* **2008,** *49*, (10), 2387-2425.
23. Bhattacharjee, P. K.; Rutledge, G. C. Electrospinning and polymer nanofibers: Process fundamentals. In *Comprehensive Biomaterials*, 2011; Vol. 1, pp 497-512.
24. Greiner, A.; Wendorff, J. H. Electrospinning: A fascinating method for the preparation of ultrathin fibers. *Angew. Chem. Int. Ed.* **2007,** *46*, (30), 5670-5703.
25. Quirós, J.; Boltes, K.; Rosal, R. Bioactive applications for electrospun fibers. *Polymer Reviews* **2016,** *56*, (4), 631-667.
26. Patil, J. V.; Mali, S. S.; Kamble, A. S.; Hong, C. K.; Kim, J. H.; Patil, P. S. Electrospinning: A versatile technique for making of 1D growth of nanostructured nanofibers and its applications: An experimental approach. *Appl. Surf. Sci.* **2017,** *423*, 641-674.
27. Dobosz, K. M.; Kuo-Leblanc, C. A.; Martin, T. J.; Schiffman, J. D. Ultrafiltration membranes enhanced with electrospun nanofibers exhibit improved flux and fouling resistance. *Industrial & Engineering Chemistry Research* **2017,** *56*, (19), 5724-5733.
28. Wang, X.; Fang, D.; Yoon, K.; Hsiao, B. S.; Chu, B. High performance ultrafiltration composite membranes based on poly(vinyl alcohol) hydrogel coating on crosslinked nanofibrous poly(vinyl alcohol) scaffold. *J. Membr. Sci.* **2006,** *278*, (1), 261-268.
29. Yoon, K.; Kim, K.; Wang, X.; Fang, D.; Hsiao, B. S.; Chu, B. High flux ultrafiltration membranes based on electrospun nanofibrous PAN scaffolds and chitosan coating. *Polymer* **2006,** *47*, (7), 2434-2441.
30. Hoover, L. A.; Schiffman, J. D.; Elimelech, M. Nanofibers in thin-film composite membrane support layers: Enabling expanded application of forward and pressure retarded osmosis. *Desalination* **2013,** *308*, 73-81.
31. Sundarrajan, S.; Balamurugan, R.; Kaur, S.; Ramakrishna, S. Potential of engineered electrospun nanofiber membranes for nanofiltration applications. *Drying Technol.* **2013,** *31*, (2), 163-169.
32. Lu, T. D.; Chen, B. Z.; Wang, J.; Jia, T. Z.; Cao, X. L.; Wang, Y.; Xing, W.; Lau, C. H.; Sun, S. P. Electrospun nanofiber substrates that enhance polar solvent separation from organic compounds in thin-film composites. *Journal of Materials Chemistry A* **2018,** *6*, (31), 15047-15056.
33. Kumeta, K.; Nagashima, I.; Matsui, S.; Mizoguchi, K. Crosslinking reaction of poly(vinyl alcohol) with poly(acrylic acid) (PAA) by heat treatment: Effect of neutralization of PAA. *J. Appl. Polym. Sci.* **2003,** *90*, (9), 2420-2427.

34. Gratzl, G.; Paulik, C.; Hild, S.; Guggenbichler, J. P.; Lackner, M. Antimicrobial activity of poly(acrylic acid) block copolymers. *Materials Science and Engineering: C* **2014,** *38*, 94-100.
35. Santiago-Morales, J.; Amariei, G.; Letón, P.; Rosal, R. Antimicrobial activity of poly(vinyl alcohol)-poly(acrylic acid) electrospun nanofibers. *Colloids and Surfaces B: Biointerfaces* **2016,** *146*, 144-151.
36. Nyström, M.; Järvinen, P. Modification of polysulfone ultrafiltration membranes with UV irradiation and hydrophilicity increasing agents. *J. Membr. Sci.* **1991,** *60*, (2), 275-296.
37. Amariei, G.; Santiago-Morales, J.; Boltes, K.; Letón, P.; Iriepa, I.; Moraleda, I.; Fernández-Alba, A. R.; Rosal, R. Dendrimer-functionalized electrospun nanofibres as dual-action water treatment membranes. *Sci. Total Environ.* **2017,** *601-602*, 732-740.
38. Jeong, S.; Kim, L. H.; Kim, S.-J.; Nguyen, T. V.; Vigneswaran, S.; Kim, I. S. Biofouling potential reductions using a membrane hybrid system as a pre-treatment to seawater reverse osmosis. *Appl. Biochem. Biotechnol.* **2012,** *167*, (6), 1716-1727.
39. Herzberg, M.; Elimelech, M. Biofouling of reverse osmosis membranes: Role of biofilm-enhanced osmotic pressure. *J. Membr. Sci.* **2007,** *295*, (1), 11-20.
40. Kessler, F.; Kühn, S.; Radtke, C.; Weibel, D. E. Controlling the surface wettability of poly(sulfone) films by UV-assisted treatment: benefits in relation to plasma treatment. *Polym. Int.* **2013,** *62*, (2), 310-318.
41. Kasemset, S.; He, Z.; Miller, D. J.; Freeman, B. D.; Sharma, M. M. Effect of polydopamine deposition conditions on polysulfone ultrafiltration membrane properties and threshold flux during oil/water emulsion filtration. *Polymer* **2016,** *97*, 247-257.
42. Bildyukevich, A. V.; Plisko, T. V.; Liubimova, A. S.; Volkov, V. V.; Usosky, V. V. Hydrophilization of polysulfone hollow fiber membranes via addition of polyvinylpyrrolidone to the bore fluid. *J. Membr. Sci.* **2017,** *524*, 537-549.
43. Kirwan, L. J.; Fawell, P. D.; van Bronswijk, W. *In situ* FTIR-ATR examination of poly(acrylic acid) adsorbed onto hematite at low pH. *Langmuir* **2003,** *19*, (14), 5802-5807.
44. Arndt, K. F.; Richter, A.; Ludwig, S.; Zimmermann, J.; Kressler, J.; Kuckling, D.; Adler, H. J. Poly(vinyl alcohol)/poly(acrylic acid) hydrogels: FT-IR spectroscopic characterization of crosslinking reaction and work at transition point. *Acta Polym.* **1999,** *50*, (11-12), 383-390.
45. Rivaton, A.; Gardette, J. L. Photodegradation of polyethersulfone and polysulfone. *Polym. Degrad. Stab.* **1999,** *66*, (3), 385-403.
46. Yamashita, T.; Tomitaka, H.; Kudo, T.; Horie, K.; Mita, I. Degradation of sulfur-containing aromatic polymers: Photodegradation of polyethersulfone and polysulfone. *Polym. Degrad. Stab.* **1993,** *39*, (1), 47-54.
47. Rupiasih, N. N.; Suyanto, H.; Sumadiyasa, M.; Wendri, N. Study of effects of low doses UV radiation on microporous polysulfone membranes in sterilization process. *Open Journal of Organic Polymer Materials* **2013,** *Vol.03No.01*, 7.
48. Jin, X.; Hsieh, Y. L. pH-responsive swelling behavior of poly(vinyl alcohol)/poly(acrylic acid) bi-component fibrous hydrogel membranes. *Polymer* **2005,** *46*, (14), 5149-5160.
49. Zhang, J.; Xu, Z.; Mai, W.; Min, C.; Zhou, B.; Shan, M.; Li, Y.; Yang, C.; Wang, Z.; Qian, X. Improved hydrophilicity, permeability, antifouling and mechanical performance of PVDF composite ultrafiltration membranes tailored by oxidized low-dimensional carbon nanomaterials. *Journal of Materials Chemistry A* **2013,** *1*, (9), 3101-3111.
50. Habimana, O.; Semião, A. J. C.; Casey, E. The role of cell-surface interactions in bacterial initial adhesion and consequent biofilm formation on nanofiltration/reverse osmosis membranes. *J. Membr. Sci.* **2014,** *454*, 82-96.
51. Yu, W.; Brown, M.; Graham, N. J. D. Prevention of PVDF ultrafiltration membrane fouling by coating MnO_2 nanoparticles with ozonation. *Scientific Reports* **2016,** *6*, 30144.
52. Rezwan, K.; Studart, A. R.; Vörös, J.; Gauckler, L. J. Change of ζ-potential of biocompatible colloidal oxide particles upon adsorption of bovine serum albumin and lysozyme. *The Journal of Physical Chemistry B* **2005,** *109*, (30), 14469-14474.
53. Gratzl, G.; Walkner, S.; Hild, S.; Hassel, A. W.; Weber, H. K.; Paulik, C. Mechanistic approaches on the antibacterial activity of poly(acrylic acid) copolymers. *Colloids and Surfaces B: Biointerfaces* **2015,** *126*, 98-105.
54. Sinn, C. G.; Dimova, R.; Antonietti, M. Isothermal titration calorimetry of the polyelectrolyte/water interaction and binding of Ca^{2+}: Effects determining the quality of polymeric scale inhibitors. *Macromolecules* **2004,** *37*, (9), 3444-3450.
55. Doyle, R. J.; Matthews, T. H.; Streips, U. N. Chemical basis for selectivity of metal ions by the Bacillus subtilis cell wall. *J. Bacteriol.* **1980,** *143*, (1), 471-480.
56. Clifton, L. A.; Skoda, M. W. A.; Le Brun, A. P.; Ciesielski, F.; Kuzmenko, I.; Holt, S. A.; Lakey, J. H. Effect of divalent cation removal on the structure of gram-negative bacterial outer membrane models. *Langmuir* **2015,** *31*, (1), 404-412.
57. Domingues, M. M.; Silva, P. M.; Franquelim, H. G.; Carvalho, F. A.; Castanho, M. A. R. B.; Santos, N. C. Antimicrobial protein rBPI21-induced surface changes on gram-negative and gram-positive bacteria. *Nanomedicine: Nanotechnology, Biology and Medicine* **2014,** *10*, (3), 543-551.
58. Rose, R. K.; Matthews, S. P.; Hall, R. C. Investigation of calcium-binding sites on the surfaces of selected gram-positive oral organisms. *Archives of Oral Biology* **1997,** *42*, (9), 595-599.
59. Thomas, K. J.; Rice, C. V. Revised model of calcium and magnesium binding to the bacterial cell wall. *BioMetals* **2014,** *27*, (6), 1361-1370.
60. Ammar, Y.; Swailes, D.; Bridgens, B.; Chen, J. Influence of surface roughness on the initial formation of biofilm. *Surf. Coat. Technol.* **2015,** *284*, 410-416.
61. Zhao, D. L.; Das, S.; Chung, T. S. Carbon quantum dots grafted antifouling membranes for osmotic power generation via pressure-retarded osmosis process. *Environmental Science & Technology* **2017,** *51*, (23), 14016-14023.

Supporting Information

Electrospun composite membranes for fouling and biofouling control

Berta Díez[†], Georgiana Amariei[†], Roberto Rosal[*]

Department of Chemical Engineering, University of Alcalá, E-28871 Alcalá de Henares, Madrid, Spain

[†] Equally contributing authors
[*] Corresponding author: roberto.rosal@uah.es, Tel.: +34918856395, Fax: +34918855088

Contents:

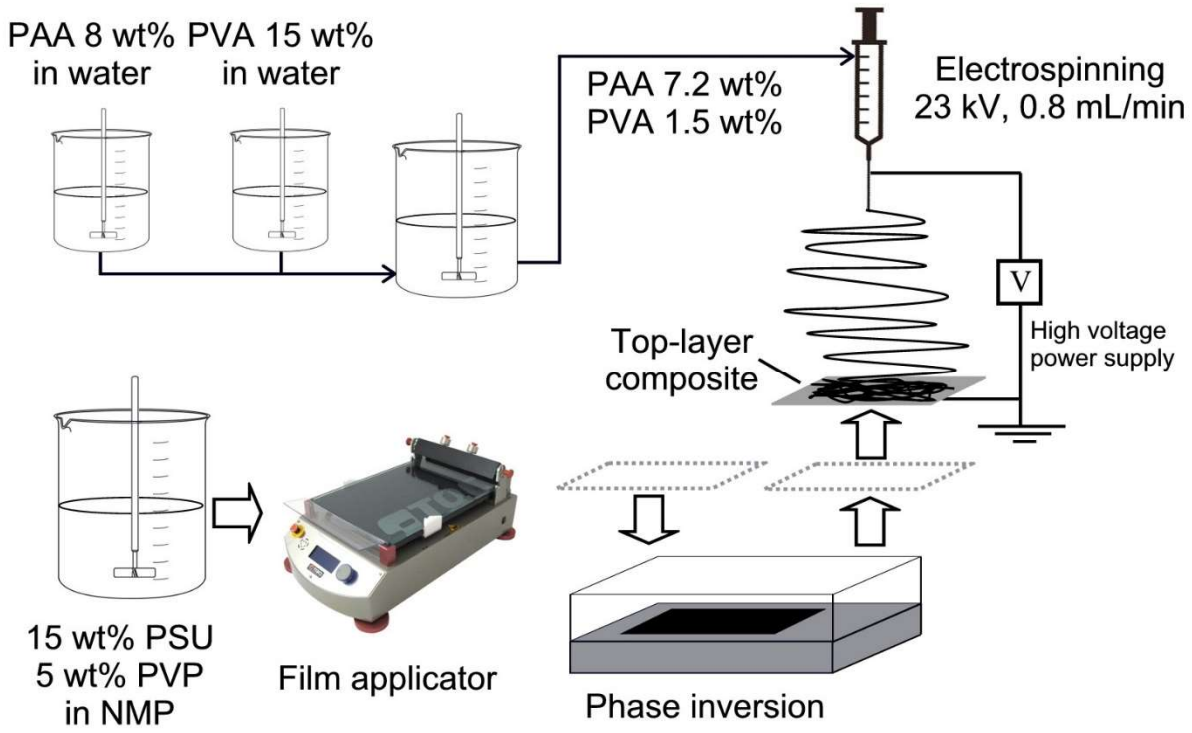

Figure S1. Scheme showing the preparation of composite membranes.

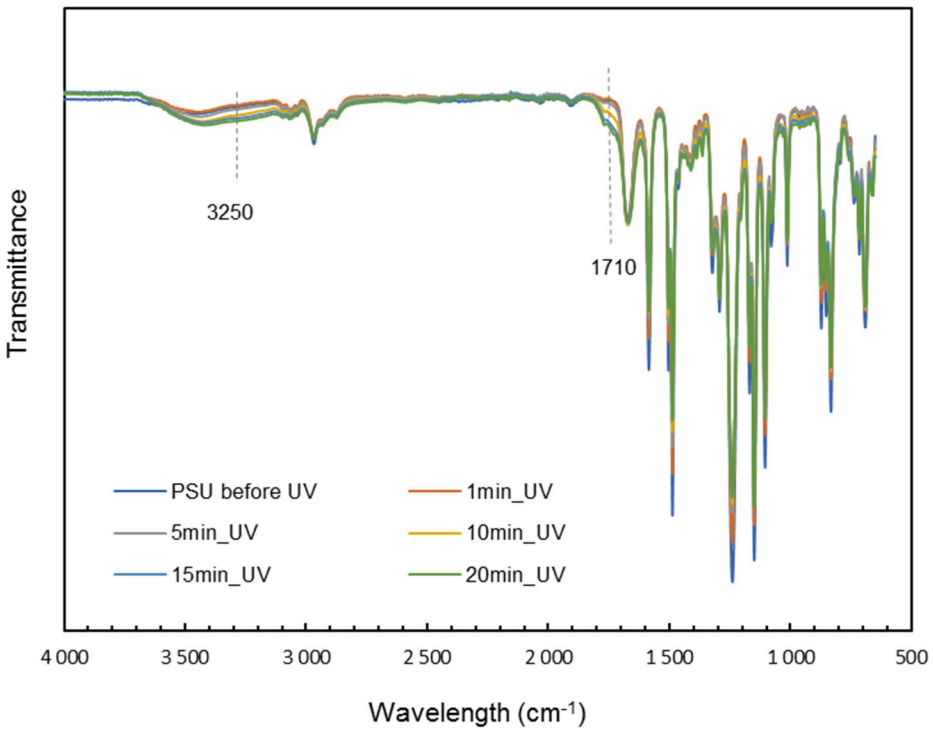

Figure S2. ATR-FTIR spectra of PSU base membranes before and after UV irradiation.

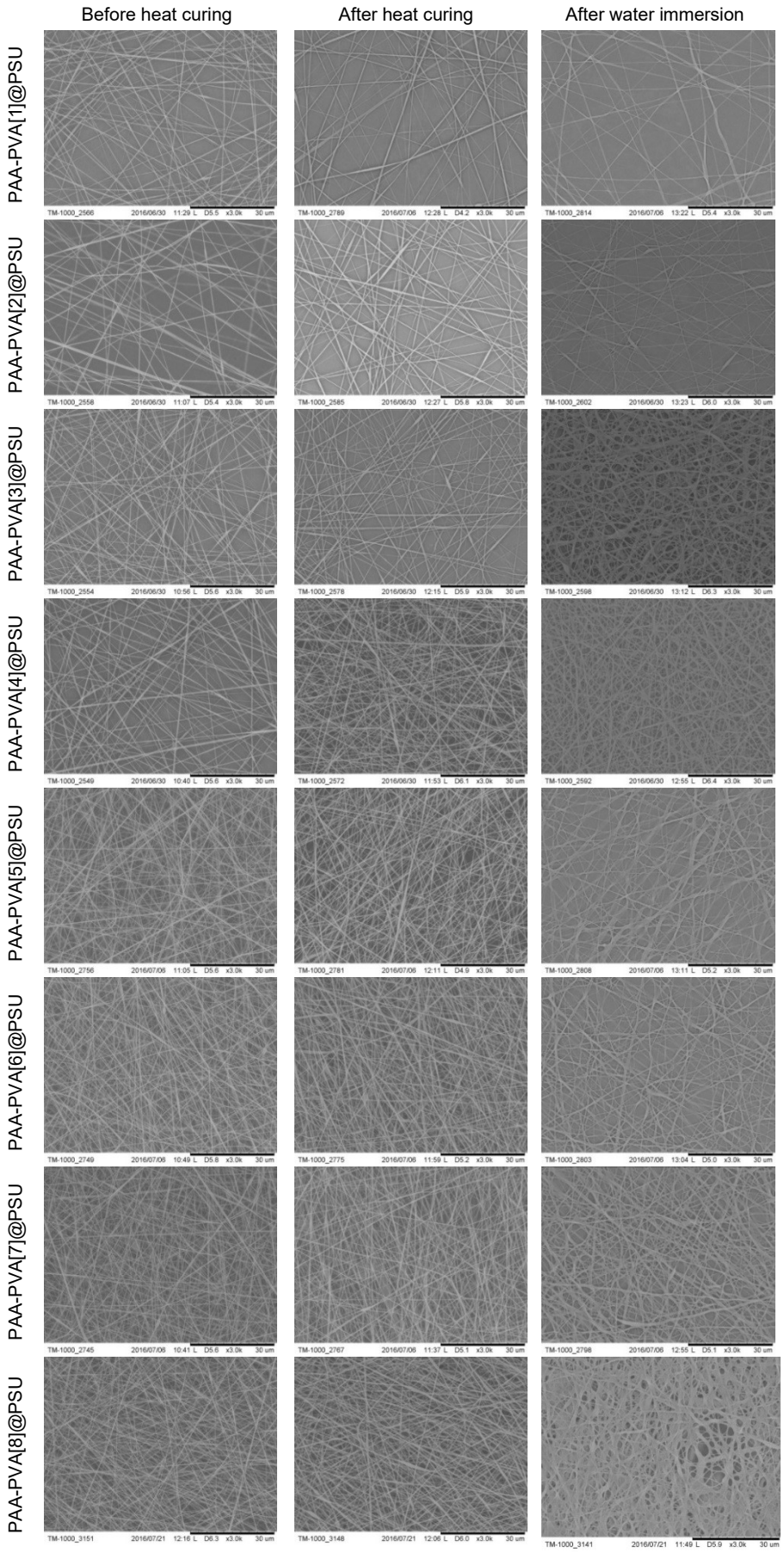

Figure S3. SEM micrographs of PAA.PVA electrospun layer (upper view) before and after heat curing and after water conditioning.

a)

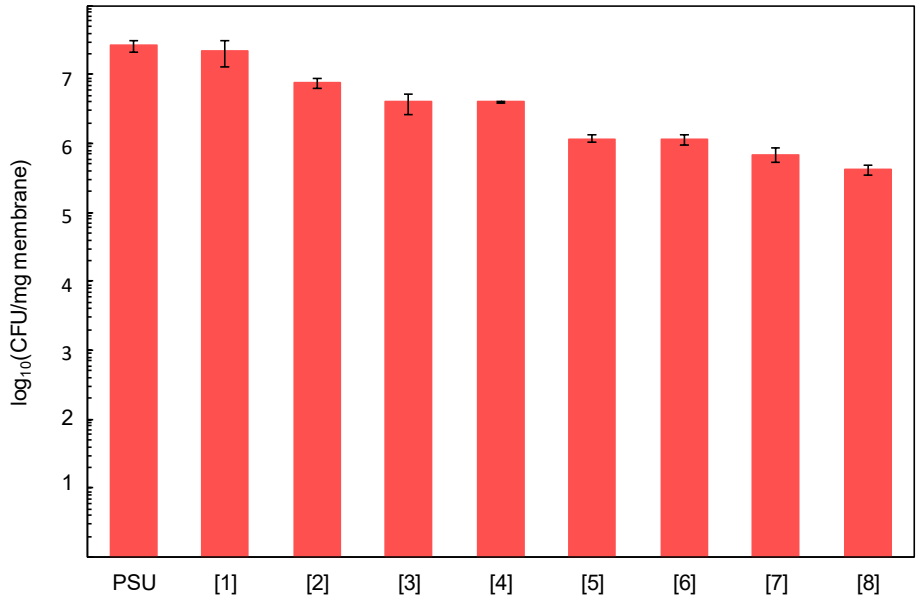

b)

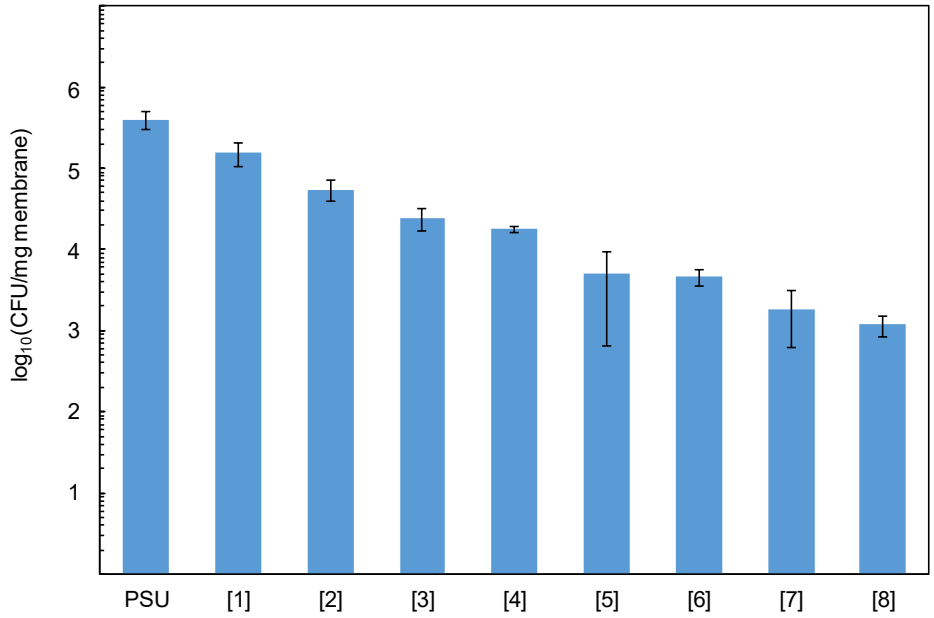

Figure S4. Colony-forming units (CFU) in the liquid media in contact with membranes for (a) *E. coli* and (b) *S. aureus*. The data correspond to the membrane compositions shown in Table 1. The cultures were kept in contact with bacteria for 20 h at 36 °C.

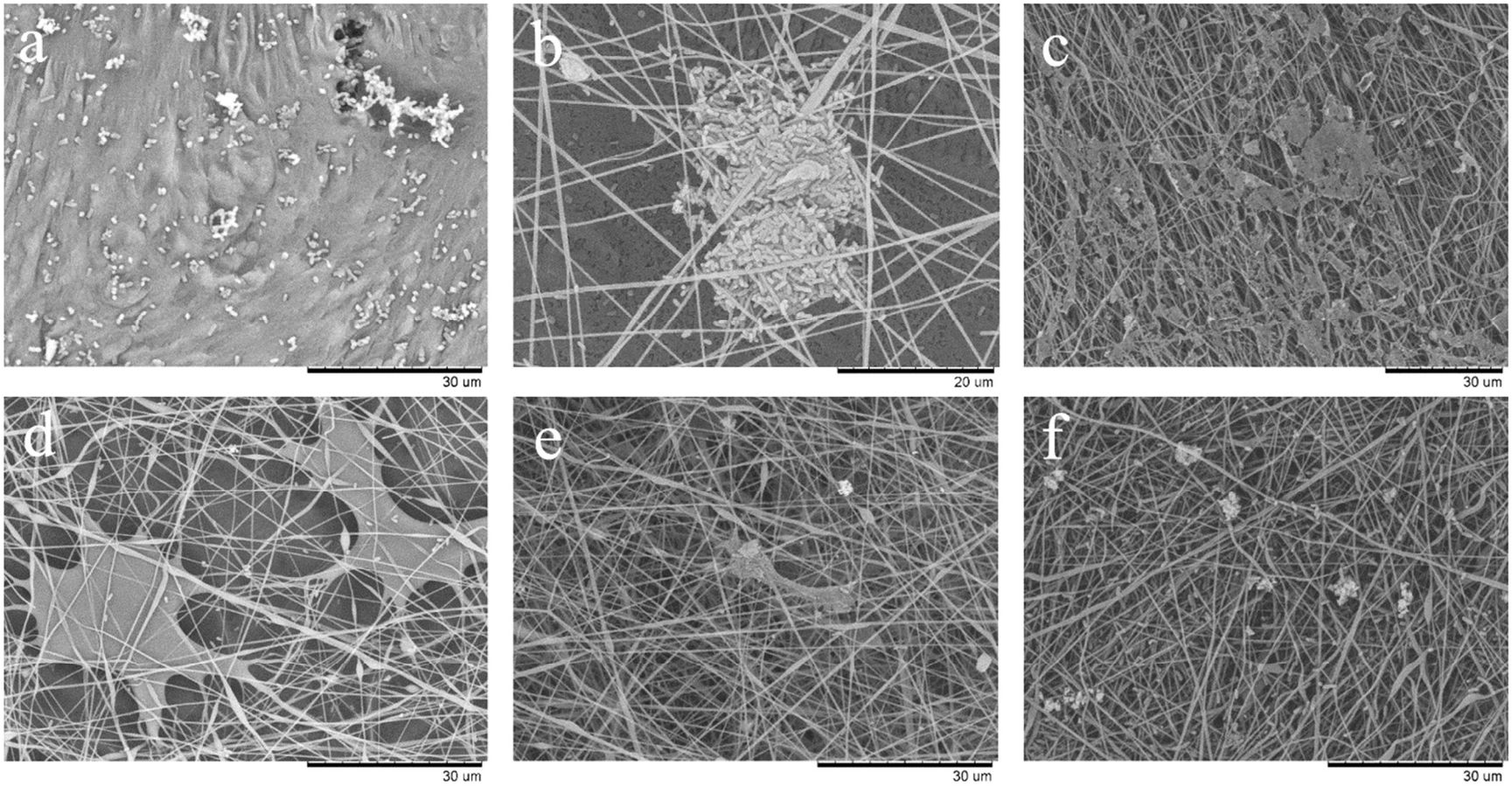

Figure S5. SEM images of the upper surface of composite membranes after 20 h contact with *E. coli* cultures at 36 °C. (a) PSU, (b) PAA-PVA[1]@PSU, (c) PAA-PVA[3]@PSU, (d) PAA-PVA[5]@PSU, (e) PAA-PVA[7]@PSU and (f) PAA-PVA[8]@PSU.

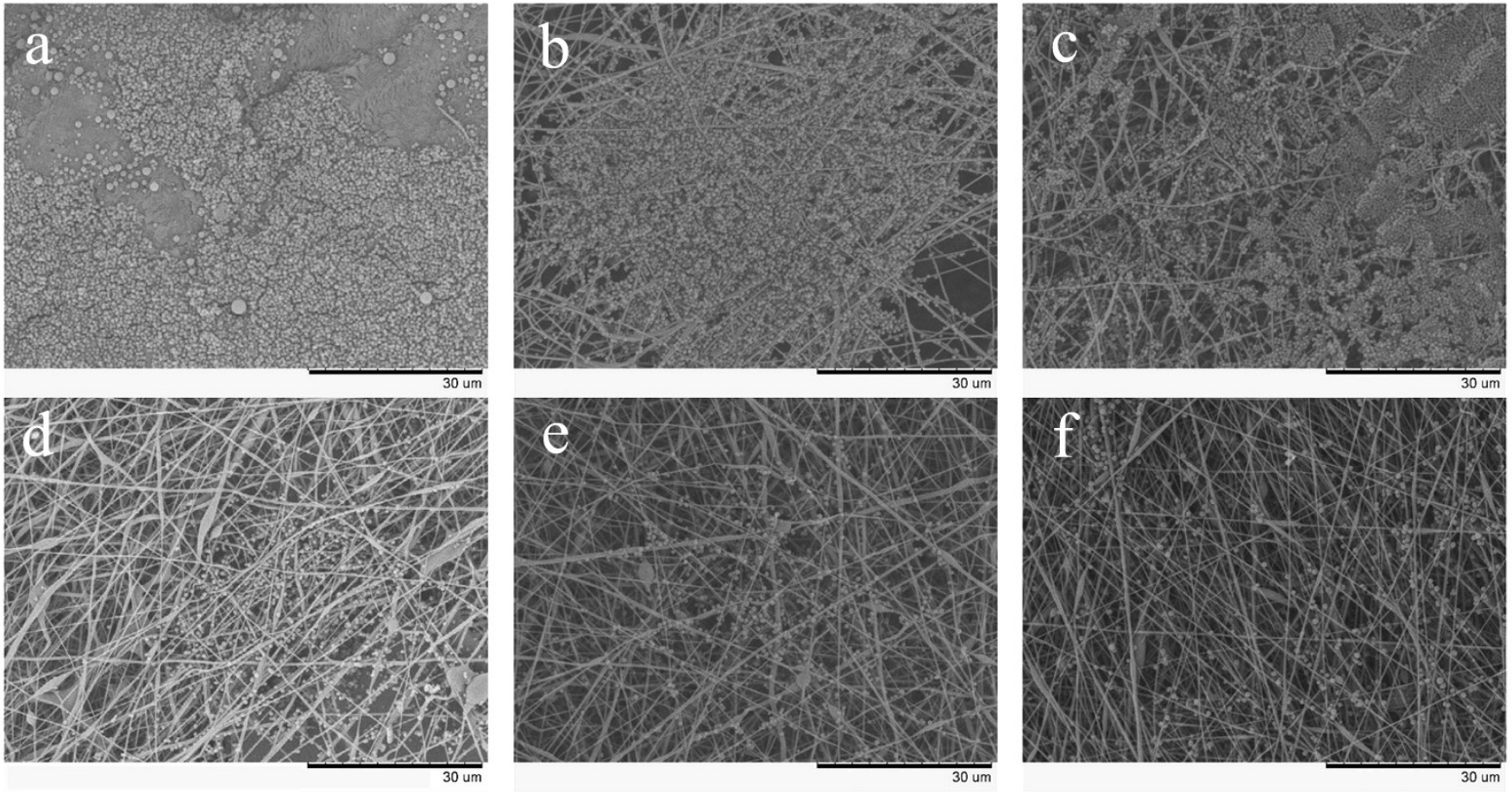

Figure S6. SEM images of the upper surface of composite membranes after 20 h contact with *S. aureus* cultures at 36 °C. (a) PSU, (b) PAA-PVA[1]@PSU, (c) PAA-PVA[3]@PSU, (d) PAA-PVA[5]@PSU, (e) PAA-PVA[7]@PSU and (f) PAA-PVA[8]@PSU.

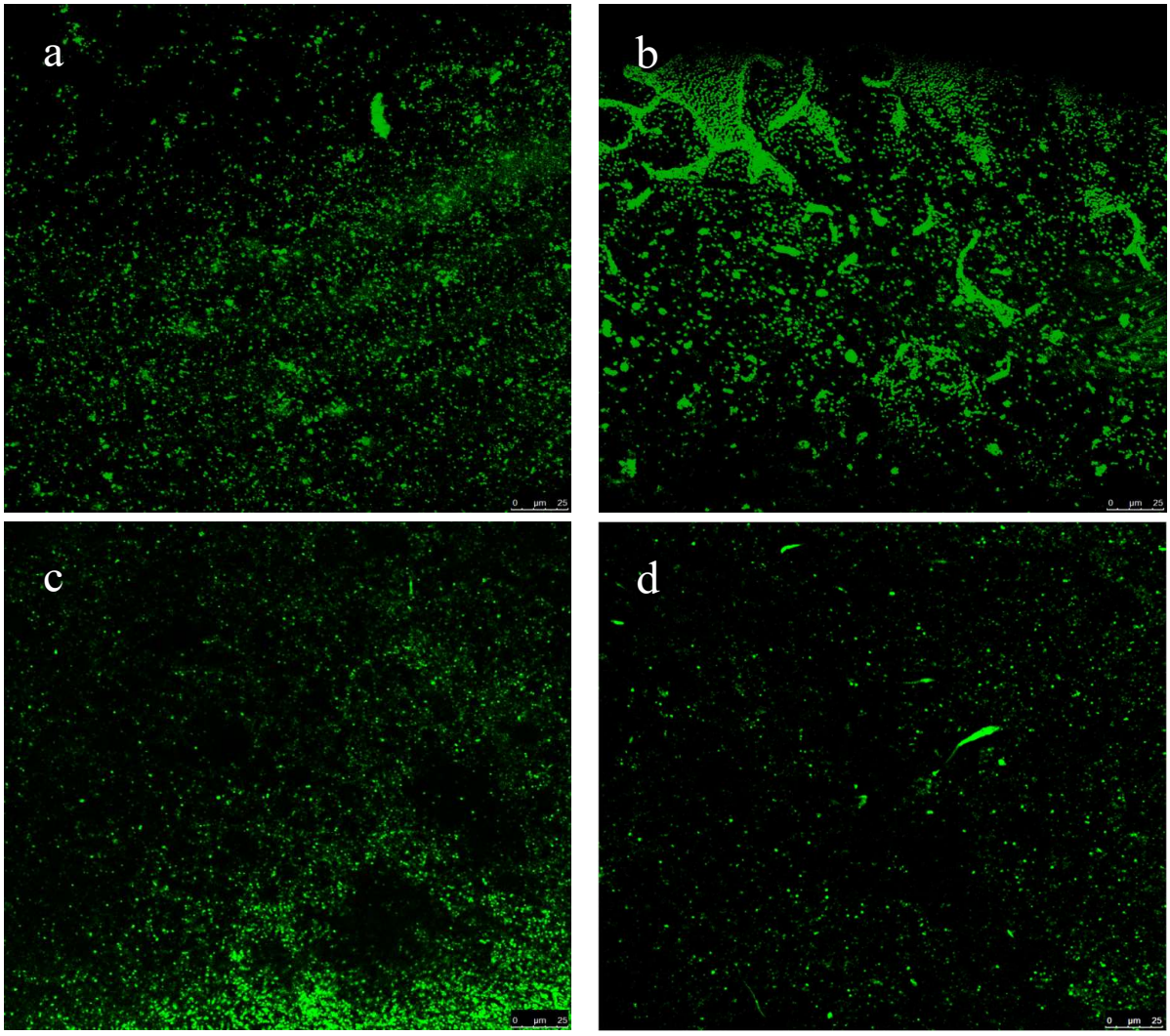

Figure S7. FilmTracer FM 1-43 Green Biofilm Cell Stain confocal micrographs of the surface of membranes exposed to *S. aureus* cultures at 36 °C for 20 h. (a) PSU, (b) PAA-PVA[1]@PSU, (c) PAA-PVA[7]@PSU and (d) PAA-PVA[8]@PSU.